Quantum and temperature effects on Davydov soliton dynamics. V. Numerical estimate of the errors introduced by the $|D_1>$ ansatz

1993 J. Phys.: Condens. Matter 5 3897

(http://iopscience.iop.org/0953-8984/5/23/016)

J. Phys.: Condens. Matter 5 (1993) 3897–3916. Printed in the UK

Quantum and temperature effects on Davydov soliton dynamics: V. Numerical estimate of the errors introduced by the $|D_1\rangle$ *ansatz*

Wolfgang Förner

Chair for Theoretical Chemistry and Laboratory of the National Foundation of Cancer Research, Friedrich-Alexander University Erlangen-Nürnberg, Egerlandstrasse 3, W-8520 Erlangen, Federal Republic of Germany

Received 21 December 1992

Abstract. For the two approximations commonly used in the Davydov soliton theory (called $|D_1\rangle$ and $|D_2\rangle$ *ansatz*), expressions for states which give the deviation of the approximation from the Schrödinger equation, i.e. $[i\hbar(\partial/\partial t) - \hat{H}]|D_1\rangle = J|\delta\rangle$, can be derived. We present numerically calculated expectation values of various operators formed with the deviation states and compare them with the corresponding expectation values formed with $\hat{H}|D_1\rangle$. Together with the fact that the basis space of the $|D_1\rangle$ state is sufficient to reproduce the exactly solvable small-polaron limit, we conclude from our results that the $|D_1\rangle$ model should be an at least qualitatively correct approximation.

1. Introduction

The basic concepts of the Davydov soliton mechanism for energy transport in proteins [1–4], as well as the different attempts to include the effects of finite temperature into the model [3–12] and the controversy about thermal stability of protein solitons has been discussed in the introduction of part II [5] of this series. Therefore we do not wish to elaborate these points here. The extensive discussion on the validity of the different *ansatz* states used in the literature [13–22] is also reviewed there [5]. A recent review of the state of art in the Davydov soliton theory was given by Scott [23].

This series of papers deals mainly with *ansatz* states which include in the theory the quantum effects on the lattice and the effects of finite temperature. In part I [19] we applied Davydov's averaged Hamiltonian method to the so-called $|D_1\rangle$ *ansatz* state [2] using the Lagrangian method advocated by Skrinjar *et al* [16] to obtain equations of motion which improve considerably the quality of the results compared with Davydov's method of using the averaged Hamiltonian as a classical Hamiltonian function [2, 14]. That is, in contrast with the previously derived equations [2, 14], the exactly solvable small-polaron limit of the theory can be reproduced with the help of these equations [16]. In [19] we demonstrated numerically that, at 300 K and for reasonable values of the parameters, travelling solitons show up in the model. Since Davydov's concept of using a thermally averaged Hamiltonian (in our case a thermally averaged Lagrangian) to obtain equations of motion was criticized as being inconsistent with statistical mechanics [24], we compared the results of several models which include the temperature in the theory with exact numerical results from quantum Monte Carlo (QMC) calculations by Wang *et al* [20] in part II [5] of this series. We found that only the averaged Hamiltonian method leads to qualitatively correct results, although

0953-8984/93/233897+20$07.50

it is quantitatively incorrect. Also in this paper we presented for the first time dynamic simulations employing the partial dressing state used by Brown and Ivic [22] at finite temperatures. However, this model does not reproduce the QMC results even quantitatively.

Therefore, in part III [25], we used the averaged Hamiltonian method to study the effects of interchain coupling present in protein α-helices at finite temperatures, following the suggestion of Scott that this coupling should stabilize the solitons compared with the one-chain case. We found that the soliton stability windows in the parameter space at 300 K for the one-chain and the three-chain cases are very similar to each other and that solitons should exist at 300 K for reasonable values of the parameters also in the three-chain case.

In an attempt to find a better model for temperature effects in the $|D_1\rangle$ *ansatz* we presented in part IV [26], soliton dynamics using a lattice with a thermal phonon population instead of an averaged Hamiltonian. However, comparison with the QMC results showed that the averaged Hamiltonian method is also superior to this model. Since at 0 K the $|D_1\rangle$ *ansatz* is still an approximation, it would be helpful to have a numerical estimate of the errors introduced by this approximate *ansatz*. Therefore we present in this paper the expectation values of several operators in the state $|\delta\rangle$ which represents the error of the $|D_1\rangle$ state if it is substituted into the time dependent Schrödinger equation: $[i\hbar(\partial/\partial t) - \hat{H}]|D_1\rangle = J|\delta\rangle$. J is one of the parameters in the Hamiltonian (see below). For an exact solution, $|\delta\rangle = 0$ would be required. We compare these expectation values with the corresponding values in the state $\hat{H}|D_1\rangle$ to obtain a numerical estimate of the errors occurring. For comparison the same is done also for the semiclassical so-called $|D_2\rangle$ *ansatz* [1]. Finally in an appendix we give a possible way to improve the quality of the *ansatz* further.

2. Method

In order to make the notation clear we repeat here the form of the Hamiltonian introduced by Davydov [1]:

$$\hat{H} = \sum_n [E_0 \hat{a}_n^+ \hat{a}_n - J(\hat{a}_n^+ \hat{a}_{n+1} + \hat{a}_{n+1}^+ \hat{a}_n) + \frac{\hat{p}_n^2}{2M} + \tfrac{1}{2} W(\hat{q}_{n+1} - \hat{q}_n)^2 + X \hat{a}_n^+ \hat{a}_n (\hat{q}_{n+1} - \hat{q}_n)]. \tag{1}$$

In equation (1) $\hat{a}_n^+$ and $\hat{a}_n$ are the usual boson creation and annihilation operators, respectively, [3], for the amide-I oscillators at sites n (figure 1). From infrared spectra the ground-state energy of an isolated amide-I oscillator can be deduced ($E_0 = 0.205$ eV). Usually, for all parameters in equation (1), site-independent mean values are used. The average value for the dipole–dipole coupling between neighbouring amide-I oscillators is $J = 0.967$ meV. The average spring constant of the hydrogen bonds is usually taken to be $W = 13$ N m^{-1}, $\hat{p}_n$ is the momentum and $\hat{q}_n$ is the position operator for unit n. The average mass M is taken to be that of myosine ($M = 114 m_p$; m_p is the proton mass). The energy of the CO stretching vibration in hydrogen bonds is a function of the length r of the hydrogen bond ($E = E_0 + Xr$). For X the experimental estimates are 35 pN and 62 pN. *Ab-initio* calculations on formamide dimers usually lead to $X = 30$–50 pN; however, with small-basis-set *ab-initio* calculations, even negative values were obtained for X (see, e.g. [22] for a review and references).

The Hamiltonian [1, 2] in a second-quantized form including disorder is given by

$$\hat{H} = \sum_n [(E_0 + E_n)\hat{a}_n^+ \hat{a}_n - J_n(\hat{a}_{n+1}^+ \hat{a}_n + \hat{a}_n^+ \hat{a}_{n+1})]$$

$$+\sum_k \hbar\omega_k\left(\hat{b}_k^+\hat{b}_k+\tfrac{1}{2}+\sum_n B_{nk}(\hat{b}_k+\hat{b}_k^+)\hat{a}_n^+\hat{a}_n\right)$$

$$B_{nk}=(X_n/\omega_k)(1/\sqrt{2\hbar\omega_k})\left(U_{n+1,k}/\sqrt{M_{n+1}}-U_{nk}/\sqrt{M_n}\right). \tag{2}$$

$\hat{b}_k^+$ and $\hat{b}_k$ are creation and annihilation operators, respectively, for acoustic phonons of wave number k. The translational mode has to be excluded from the summation. Note that, in the simulations presented, we again use the asymmetric interaction model where only the coupling of the oscillator n to the hydrogen bond between n and $n+1$ in which the oscillator takes part is considered. ω_k denotes the eigenfrequency of the normal mode k and **U** contains the normal mode coefficients. ω and **U** are obtained by numerical diagonalization of the matrix **V** with the elements

$$\begin{aligned}V_{nm}=\{&[W_n(1-\delta_{nN})+W_{n-1}(1-\delta_{n1})]\delta_{nm}-W_n(1-\delta_{nN})\delta_{m,n+1}\\&-W_{n-1}(1-\delta_{n1})\delta_{m,n-1}\}(M_nM_m)^{-1/2}.\end{aligned} \tag{3}$$

The form of **V** implies that we use free chain ends and N units.

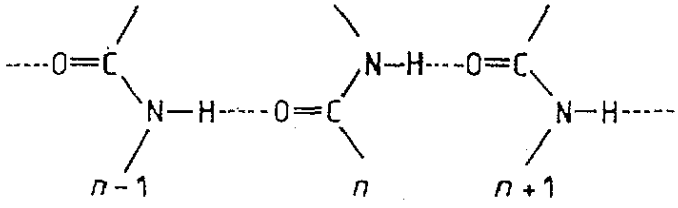

Figure 1. Schematic picture of a hydrogen-bonded channel in a protein.

The $|D_1\rangle$ *ansatz* state on which most of the work reported in this series of papers is based is ($|0\rangle_p$ denotes the phonon vacuum, and $|0\rangle_e$ the exciton vacuum)

$$\begin{aligned}&|D_1\rangle=\sum_n a_n(t)a_n^+|0\rangle_e|\beta_n\rangle \qquad |\beta_n\rangle=\hat{U}_n|0\rangle_p\\&\hat{U}_n=\prod_k\hat{U}_{nk} \qquad \hat{U}_{nk}=\exp[b_{nk}(t)\hat{b}^+-b_{nk}^*(t)\hat{b}_k]\end{aligned} \tag{4}$$

where the $b_{nk}(t)$ are the coherent-state amplitudes and $|a_n(t)|^2$ is the probability of finding a quantum of the amide-I vibration at site n. The equations of motion derived from this *ansatz* with the help of the Euler–Lagrange method, time-dependent variational principle or Heisenberg's operator method are given (for $T=0$ K) in [16] and the preceding papers of this series, so we shall not repeat them here. It was shown by Skrinjar *et al* [16] that, from these equations, one can derive that

$$i\hbar(\partial/\partial t)|D_1\rangle=J((\hat{H}/J)|D_1\rangle+|\delta\rangle) \tag{5}$$

holds. We introduce a state

$$|\chi\rangle=\sum_n\left(xa_{n+1}|\beta_{n+1}\rangle-\gamma_n|\beta_n\rangle-a_{n-1}|\beta_{n-1}\rangle-\sum_k\alpha_{nk}\hat{U}_n\hat{b}_k^+|0\rangle_p\right)\hat{a}_n^+|0\rangle_e. \tag{6}$$

By separate evaluation of

$$i\hbar(\partial/\partial t)|D_1\rangle \qquad \text{and} \qquad \hat{H}|D_1\rangle \tag{7}$$

and with the help of the equations of motion it can be easily shown that if one sets

$$\begin{aligned} &x = 1 \qquad \gamma_n = D_{n,n+1}a_{n+1} - D_{n,n-1}a_{n-1} \\ &\alpha_{nk} = a_{n+1}(b_{n+1,k} - b_{nk})D_{n,n+1} + a_{n-1}(b_{n-1,k} - b_{nk})D_{n,n-1} \end{aligned} \tag{8}$$

$|\chi\rangle = |\delta\rangle$ holds. Further if we set

$$\begin{aligned} &x = -1 \qquad \gamma_n = -\left(\sum_k \hbar\omega_k[|b_{nk}|^2 + \tfrac{1}{2} + B_{nk}(b_{nk} + b_{nk}^*)] + E_0\right)\frac{a_n}{J} \\ &\alpha_{nk} = -\hbar\omega_k(B_{nk} + b_{nk})a_n/J \end{aligned} \tag{9}$$

$|\chi\rangle = (\hat{H}/J)|D_1\rangle$ is obtained where the overlaps of the Glauber coherents phonon states are given by

$$D_{nm} = \langle\beta_n|\beta_m\rangle = \exp\left(-\tfrac{1}{2}\sum_k(|b_{nk} - b_{mk}|^2 + b_{mk}^*b_{nk} - b_{mk}b_{nk}^*)\right). \tag{10}$$

Further one can easily show that the error $|\delta\rangle$ is orthogonal to $|D_1\rangle$, that the energy expectation value for $|D_1\rangle$ is equal to the exact energy of the system and finally that

$$\langle D_1|i\hbar\,\partial/\partial t - \hat{H}|D_1\rangle = 0 \tag{11}$$

holds [16].

In this work we shall calculate the expectation values

$$\langle\chi|\chi\rangle \qquad \langle\chi|\hat{a}_n^+\hat{a}_n|\chi\rangle \qquad \langle\chi|\hat{b}_k|\chi\rangle \qquad \langle\chi|\hat{p}_n|\chi\rangle \qquad \langle\chi|\hat{q}_n|\chi\rangle \tag{12}$$

and compare their numerical values for $(\hat{H}/J)|D_1\rangle$ and the error $|\delta\rangle$ to obtain a feeling of the errors introduced by the approximate nature of the $|D_1\rangle$ *ansatz*. Note that, in contrast with the usually applied procedure, we do *not* eliminate terms in the equations of motion which are products of a site-independent constant multiplied by a_n as a phase factor at the a-values. In appendix 1 we give some commutation relations and expectation values of various operators which are necessary to derive the expressions for the values listed above.

First of all we shall compute projections of the state $|\chi\rangle$ on our non-orthogonal basis states:

$$|n^+\rangle \equiv \hat{a}_n^+|0\rangle_e|\beta_{n+1}\rangle \qquad |n\rangle \equiv \hat{a}_n^+|0\rangle_e|\beta_n\rangle \qquad |n^-\rangle \equiv \hat{a}_n^+|0\rangle_e|\beta_{n-1}\rangle$$

$$|n,k\rangle \equiv \hat{a}_n^+|0\rangle_e\hat{U}_n\hat{b}_k^+|0\rangle_p$$

$$\rightarrow |\chi\rangle = \sum_n\left(xa_{n+1}|n^+\rangle - \gamma_n|n\rangle - a_{n-1}|n^-\rangle - \sum_k\alpha_{nk}|n,k\rangle\right). \tag{13}$$

From this we easily obtain the projections

$$\langle n^+|\chi\rangle = xa_{n+1} - \gamma_nD_{n+1,n} - a_{n-1}D_{n+1,n-1} - \sum_k\alpha_{nk}(b_{n+1,k}^* - b_{nk}^*)D_{n+1,n}$$

$$\begin{aligned} &\langle n|\chi\rangle = xa_{n+1}D_{n,n+1} - \gamma_n - a_{n-1}D_{n,n-1} \\ &\langle n^-|\chi\rangle = xa_{n+1}D_{n-1,n+1} - \gamma_nD_{n-1,n} - a_{n-1} - \sum_k\alpha_{nk}(b_{n-1,k}^* - b_{nk}^*)D_{n-1,n} \end{aligned} \tag{14}$$

$$\langle n,k|\chi\rangle = xa_{n+1}(b_{n+1,k} - b_{nk})D_{n,n+1} - a_{n-1}(b_{n-1,k} - b_{nk})D_{n,n-1} - \alpha_{nk}.$$

The norm of our state can be computed using the expectation values given in appendix 1:

$$\langle\chi|\chi\rangle = \sum_n \Bigg[2\,\mathrm{Re}\Bigg(- x a^*_{n+1} a_{n-1} D_{n+1,n-1} - \gamma_n (x a^*_{n+1} D_{n+1,n} - a^*_{n-1} D_{n-1,n}) + \sum_k \alpha_{nk} (b^*_{n-1,k} - b^*_{nk}) D_{n-1,n} a^*_{n-1} - x \sum_k \alpha_{nk} (b^*_{n+1,k} - b^*_{nk}) D_{n+1,n} a^*_{n+1} \Bigg) + |a_{n+1}|^2 + |a_{n-1}|^2 + |\gamma_n|^2 + \sum_k |\alpha_{nk}|^2 \Bigg]. \tag{15}$$

A numerical comparison of the norm of our two states will give us an idea of how important the error made by the *ansatz* in comparison with $(\hat{H}/J)|D_1\rangle$ will be. Further we are interested in the expectation value of the number operator for the amide-I oscillators in the two states under investigation. This value can be computed with the formula

$$\begin{aligned}\langle\chi|\hat{a}^+_n \hat{a}_n|\chi\rangle = {} & x a^*_{n+1} \Bigg(x a_{n+1} - \gamma_n D_{n+1,n} - a_{n-1} D_{n+1,n-1} - \sum_k \alpha_{nk} (b^*_{n+1,k} - b^*_{nk}) D_{n+1,n} \Bigg) \\ & - \gamma^*_n (x a_{n+1} D_{n,n+1} - \gamma_n - a_{n-1} D_{n,n-1}) \\ & - a^*_{n-1} \Bigg(x a_{n+1} D_{n-1,n+1} - \gamma_n D_{n-1,n} - a_{n-1} - \sum_k \alpha_{nk} (b^*_{n-1,k} - b^*_{nk}) D_{n-1,n} \Bigg) \\ & - \sum_k \alpha^*_{nk} [x a_{n+1} (b_{n+1,k} - b_{nk}) D_{n,n+1} - a_{n-1} (b_{n-1,k} - b_{nk}) D_{n,n-1} - \alpha_{nk}].\end{aligned} \tag{16}$$

By rearranging the different terms, one can easily show that this expectation value is a real quantity as one expects. The numerical evaluation of this expectation value gives an idea of how large the errors in $|a_n(t)|^2$ when calculated with the $|D_1\rangle$ approximation might be. The expectation values of the phonon annihilation operators are given by

$$\begin{aligned}\langle\chi|\hat{b}_k|\chi\rangle = \sum_n \Bigg\{ & x a^*_{n+1} \Bigg[x b_{n+1,k} a_{n+1} - b_{nk} D_{n+1,n} \gamma_n - b_{n-1,k} D_{n+1,n-1} a_{n-1} \\ & - \Bigg(\alpha_{nk} + \sum_{k'} \alpha_{nk'} (b^*_{n+1,k'} - b^*_{nk'}) b_{nk} \Bigg) D_{n+1,n} \Bigg] \\ & - \gamma^*_n (x b_{n+1,k} D_{n,n+1} a_{n+1} - b_{nk} \gamma_n - b_{n-1,k} D_{n,n-1} a_{n-1} - \alpha_{nk}) \\ & - a^*_{n-1,k} \Bigg[x b_{n+1,k} D_{n-1,n+1} a_{n+1} - b_{nk} D_{n-1,n} \gamma_n - b_{n-1,k} a_{n-1} \\ & - \Bigg(\alpha_{nk} - \sum_{k'} \alpha_{nk'} (b^*_{n-1,k'} - b^*_{nk'}) b_{nk} \Bigg) D_{n-1,n} \Bigg] \\ & - \sum_{k'} \alpha^*_{nk'} [x (b_{n+1,k'} - b_{nk'}) b_{n+1,k} D_{n,n+1} a_{n+1} \\ & - (b_{n-1,k'} - b_{nk'}) b_{n-1,k} D_{n,n-1} a_{n-1} - b_{nk} \alpha_{nk'}] \Bigg\}.\end{aligned} \tag{17}$$

To check our formula for errors we derived independently the corresponding expression for the expectation values of the phonon creation operators and verified that

$$\langle\chi|\hat{b}_k|\chi\rangle = (\langle\chi|\hat{b}_k^+|\chi\rangle)^* \tag{18}$$

holds. From this we can finally compute the expectation values of momentum and displacement operators in our states:

$$\begin{aligned}\langle\chi|\hat{q}_n|\chi\rangle &= \sum_k \sqrt{(2\hbar/M\omega_k)}U_{nk}\,\mathrm{Re}(\langle\chi|\hat{b}_k|\chi\rangle)\\ \langle\chi|\hat{p}_n|\chi\rangle &= \sum_k \sqrt{2\hbar M\omega_k}U_{nk}\,\mathrm{Im}(\langle\chi|\hat{b}_k|\chi\rangle).\end{aligned} \tag{19}$$

For comparison we give in appendix 2 the corresponding expressions for the simpler $|D_2\rangle$ approximation, in which the lattice is treated classically. In section 3 we discuss numerical applications of these results.

3. Results and discussion

3.1. The $|D_1\rangle$ approximation

We have calculated numerically the above-derived expectation values and projections for four pairs of (X, W) values, namely (X = 50 pN, W = 10 N m^{-1}), (X = 150 pN, W = 10 N m^{-1}), (X = 50 pN, W = 50 N m^{-1}) and (X = 150 pN, W = 50 N m^{-1}). Since the numerical results were in all cases essentially similar, concerning the comparison between expectation values in the state $(\hat{H}/J)|D_1\rangle$ and the deviation $|\delta\rangle$, we concentrate the discussion on one of the parameter values. We have chosen X = 150 pN and W = 10 N m^{-1} since in this case a travelling soliton is present in the system which starts to disperse after reflection at the chain end, as figure 2 shows, where we present the time evolution of $|a_n(t)|^2$, the lattice displacements $q_n(t)$ and the lattice momenta $p_n(t)$.

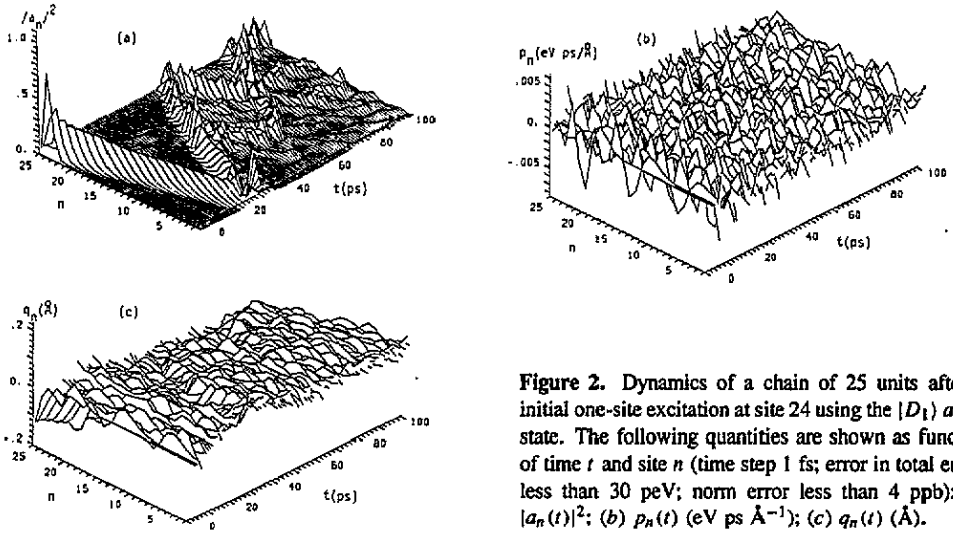

Figure 2. Dynamics of a chain of 25 units after an initial one-site excitation at site 24 using the $|D_1\rangle$ *ansatz* state. The following quantities are shown as functions of time t and site n (time step 1 fs; error in total energy less than 30 peV; norm error less than 4 ppb): (*a*) $|a_n(t)|^2$; (*b*) $p_n(t)$ (eV ps Å^{-1}); (*c*) $q_n(t)$ (Å).

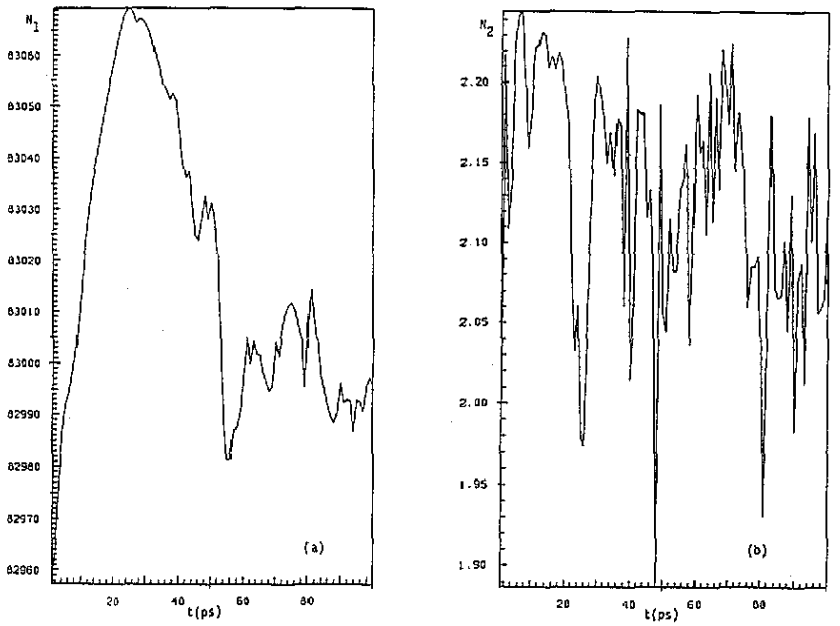

Figure 3. Time evolution of (*a*) the norm N of the state $(\hat{H}/J)|D_1\rangle$ (N_1) and (*b*) the norm of the deviation $|\delta\rangle$ (N_2).

Figures 3(*a*) and 3(*b*) show the norm N_1 of the state $(\hat{H}/J)|D_1\rangle$ and the norm N_2 of the deviation $|\delta\rangle$, respectively. It is clear from the figure that the norm of the deviation is completely negligible, being five orders of magnitude smaller than that of $(\hat{H}/J)|D_1\rangle$. Also the norm of the deviation shows no tendency to increase with time but has a strongly oscillatory character. Figure 4 shows the expectation values discussed above for the two states. Figure 4(*a*) shows the expectation values of the number operators for the amide-I oscillators as functions of site and time. Also here the values for the deviation are negligible compared with those for $(\hat{H}/J)|D_1\rangle$. In this case they are roughly four orders of magnitude smaller. Both expectation values have the same form as the time evolution of the expectation values of the number operators in the $|D_1\rangle$ state itself. The same observation holds for the expectation values of the phonon annihilation operators (real part in figure 4(*b*), and imaginary part in figure 4(*c*)). However, in this case the difference is even larger, namely five orders of magnitude. In the case of the expectation value of the momentum operators the difference is again smaller by four orders of magnitude (figure 4(*d*)), and for the displacement operators (figure 4(*e*)) by five orders of magnitude. Thus it seems that the deviations of the $|D_1\rangle$ state which result from exact solution of the time-dependent Schrödinger equation are in terms of the expectation values of the different relevant operators in the two states on the right-hand side of

$$i(\hbar/J)(\partial/\partial t)|D_1\rangle = (\hat{H}/J)|D_1\rangle + |\delta\rangle \tag{20}$$

not large and are in fact negligible, being for $|\delta\rangle$ four to five orders of magnitude smaller than for the state $(\hat{H}/J)|D_1\rangle$. Although this is not a direct measure of the errors introduced into the corresponding expectation values of the wavefunction itself, it gives at least some confidence in the numerical results of $|D_1\rangle$ dynamics. Note that the absolute values of the

expectation values formed with the deviation state can be obtained by multiplication by $J^2 = 9.35 \times 10^{-7}$ eV^2, since the deviation from the Schrödinger equation is $J|\delta\rangle$. In our calculations we have used $|\delta\rangle$ and $(\hat{H}/J)|D_1\rangle$ in order to obtain dimensionless states.

Now we turn to the projections of the two states on the right-hand side of equation (20) on the different basis states in their expansions. It is easy to verify that $\langle n|\delta\rangle = 0$ holds; thus it is also not necessary to discuss $\langle n|(\hat{H}/J)|D_1\rangle$, since our state is exact in this direction. For completeness we show the real and imaginary parts of $\langle n|(\hat{H}/J)|D_1\rangle$ in figure 5(*a*). In figures 5(*b*) and 5(*c*) we show the real and imaginary parts, respectively, of the projections of our two states on $|n^-\rangle$. We recognize immediately that in these directions the deviation is two orders of magnitude smaller than the amplitudes of $(\hat{H}/J)|D_1\rangle$. The situations for the projections in the $|n^+\rangle$ direction are very similar, as figures 5(*d*) and 5(*e*) show. One sees that, while $\langle n^{\pm}|(\hat{H}/J)|D_1\rangle$ is large when the amide-I excitation probability is large, the deviation spreads over the whole chain, however, being also more pronounced at the amide-I excitation sites. We give only two examples of the huge amount of data for the projections on the $|n, k\rangle$ basis states. In figure 5(*f*) we show the real part of the projection in the direction $|n, 1\rangle$ where $k = 1$ denotes the lowest non-zero phonon frequency. We see that in this case the deviation can be even twice the projection of $(\hat{H}/J)|D_1\rangle$ in this direction. However, in absolute values both contributions are three orders of magnitude smaller than those of the previously discussed directions and thus entirely negligible. For all higher phonon frequencies the errors are typically smaller by factors between 2 and 10 than the projections of $(\hat{H}/J)|D_1\rangle$; however, also there the latter are small enough to be negligible. As an example we show the real part of the projections in the $|n, 5\rangle$ direction in figure 5(*g*). Thus altogether it seems that the deviation of the $|D_1\rangle$-state solutions fulfil the time-dependent Schrödinger equation to quite good accuracy. In directions where the deviations are relatively large the whole contribution is negligibly small compared with the contributions in other directions. Also here the projections have to be multiplied by $J = 9.67 \times 10^{-4}$ eV, since the deviation from the Schrödinger equation is $J|\delta\rangle$. Further the deviation evolves proportional to J from the small-polaron limit ($J = 0$) where the $|D_1\rangle$ *ansatz* gives the exact solution.

3.2. The $|D_2\rangle$ approximation

The equations of motion as well as the necessary expectation values for the error are derived in appendix 2. An interesting and, to our knowledge, never reported feature of the $|D_2\rangle$ model is the extreme dependence of the soliton stability on the boundary conditions. If one uses free chain ends instead of the commonly applied fixed (i.e. a_1, a_N, q_1, q_N, p_1 and p_N are not allowed to change during the simulation) or cyclic ends, the soliton stability window concerning the parameter X is drastically reduced, as figure 6 shows. While travelling solitons appear roughly between $X = 30$ pN and $X = 80$ pN for a fixed boundary, travelling solitons show up only from $X = 60$ pN for the free boundary (with $W = 10$ N m^{-1}) and already from $X = 80$ pN the excitation becomes pinned at the chain end.

Since in the case of the $|D_2\rangle$ state the basis space is smaller than for the $|D_1\rangle$ state, one would expect the deviations from the Schrödinger equation to be larger. However, also here this deviation is minimized by the time-dependent variational principle, which is completely equivalent to the Lagrangian method used in appendix 2 for derivation of the equations of motion. Therefore the difference between the expectation values of the operators in the states $(\hat{H}/J)|D_2\rangle$ and $|\lambda\rangle$ (see appendix 2) is indeed mostly smaller than in the states $(\hat{H}/J)|D_1\rangle$ and $|\delta\rangle$, but it is not as pronounced as one would expect. Also the expectation values formed with $|\lambda\rangle$ are themselves larger than those discussed above,

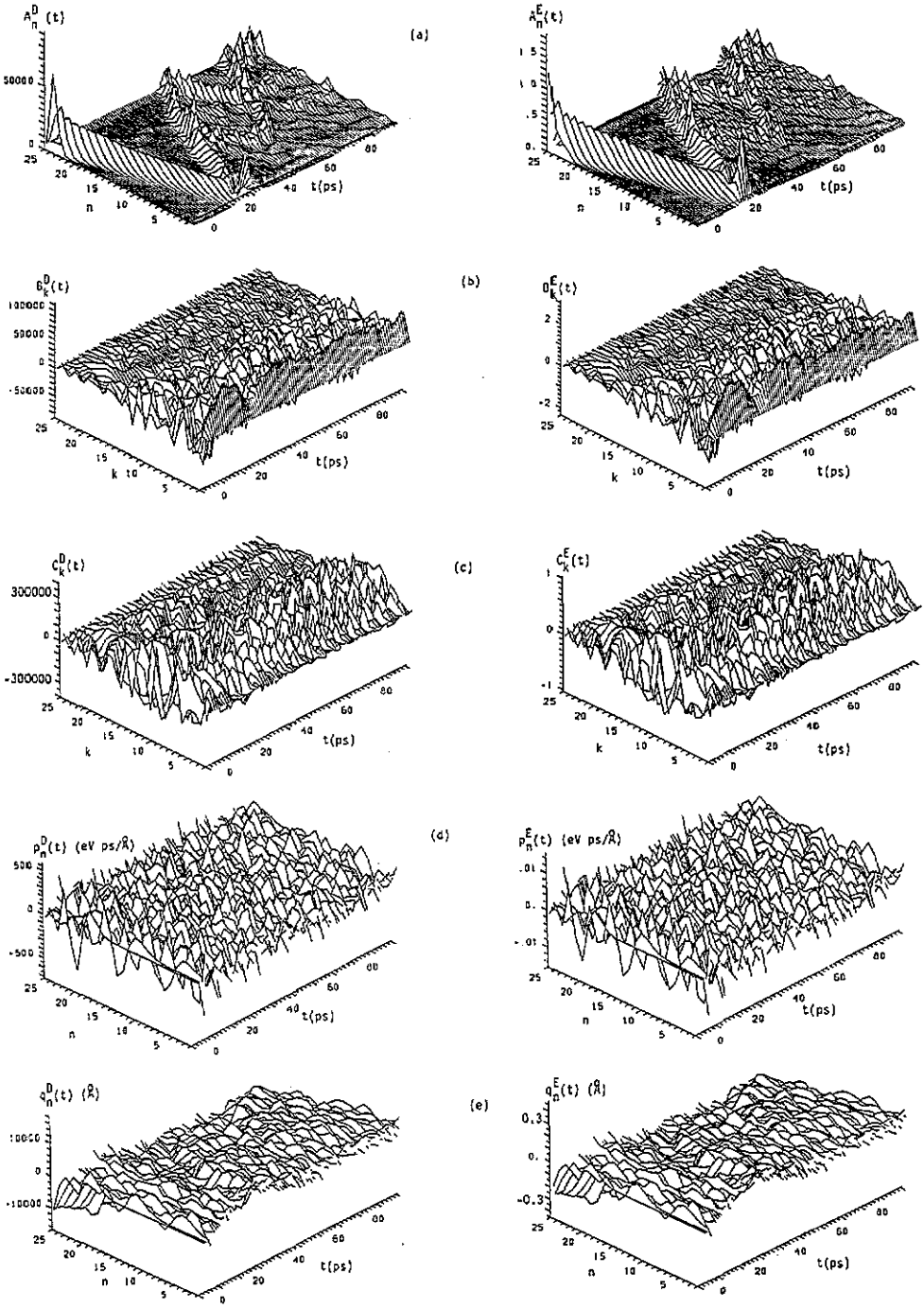

Figure 4. Expectation values of several operators in the state $(\hat{H}/J)|D_1\rangle$ (denoted by D) and in the deviation $|\delta\rangle$ (denoted by E): (*a*) number operators $A_n^{\mathrm{D}}(t)$ and $A_n^{\mathrm{E}}(t)$ for the amide-I oscillators as functions of site n and time t; (*b*) phonon annihilation operators (real parts $B_k^{\mathrm{D}}(t)$ and $B_k^{\mathrm{E}}(t)$) as functions of wavenumber k and time t; (*c*) phonon annihilation operators (imaginary parts $C_k^{\mathrm{D}}(t)$ and $C_k^{\mathrm{E}}(t)$) as functions of wavenumber k and time t; (*d*) momentum operators $p_n^{\mathrm{D}}(t)$ and $p_n^{\mathrm{E}}(t)$ as functions of site n and time t; (*e*) displacement operators $q_n^{\mathrm{D}}(t)$ and $q_n^{\mathrm{E}}(t)$ as functions of site n and time t.

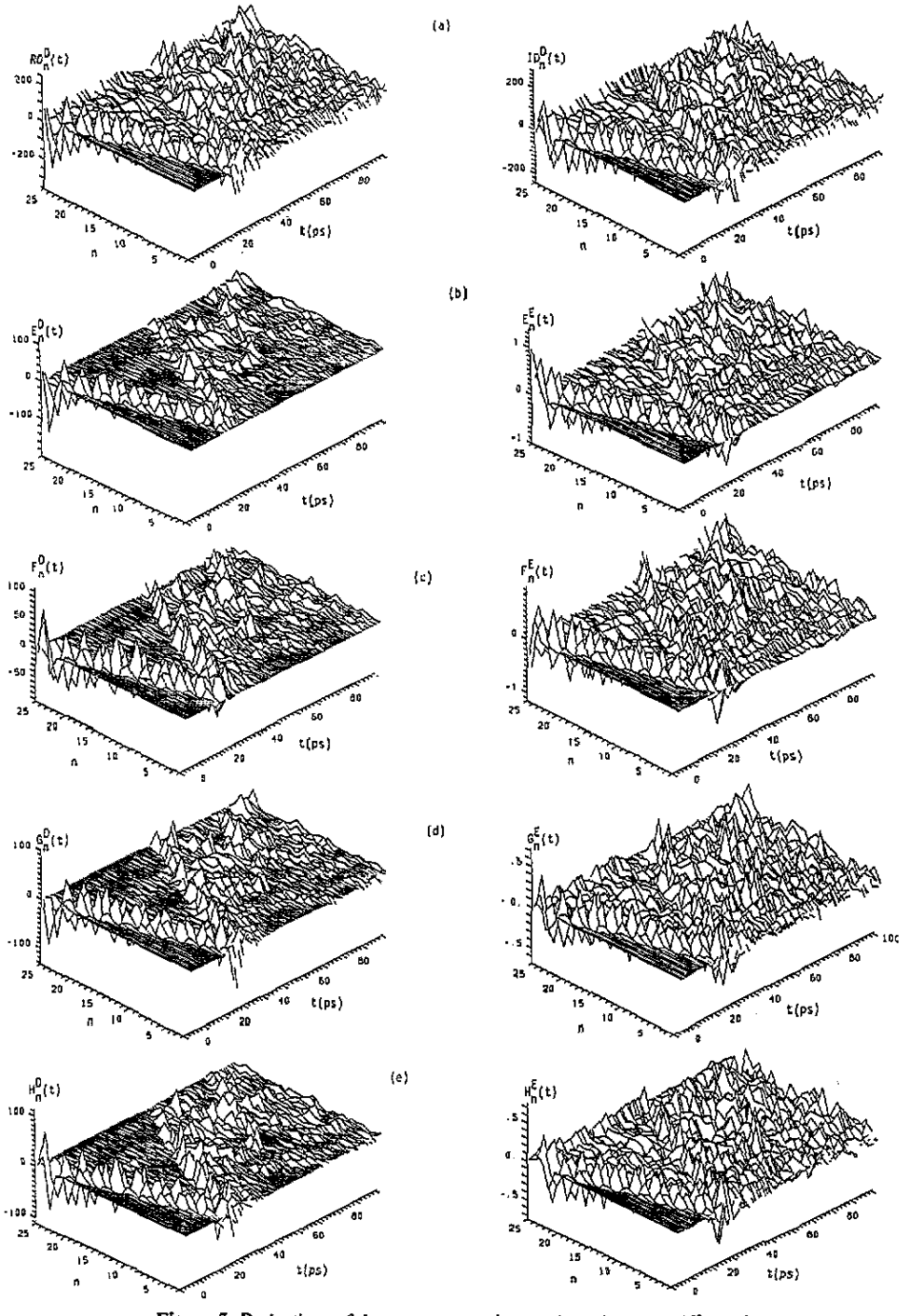

Figure 5. Projections of the two states under consideration onto different basis functions D again denotes the state $\langle \hat{H}/J|D_1\rangle$ and E the deviation $|\delta\rangle$ as functions of site and time ($|D_1\rangle$ state): (*a*) real part $\mathrm{R}D_n^D(t)$ and imaginary part $\mathrm{I}D_n^D(t)$ of $\langle n|\langle \hat{H}/J\rangle|D_1\rangle$ (note that here $\langle n|\delta\rangle = 0$ holds); (*b*) real parts of $\langle n^-|\langle \hat{H}/J\rangle|D_1\rangle$ ($E_n^D(t)$) and $\langle n^-|\delta\rangle$ ($E_n^E(t)$); (*c*) imaginary parts of $\langle n^-|\langle \hat{H}/J\rangle|D_1\rangle$ ($F_n^D(t)$) and $\langle n^-|\delta\rangle$ ($F_n^E(t)$); (*d*) real parts of $\langle n^+|\langle \hat{H}/J\rangle|D_1\rangle$ ($G_n^D(t)$) and $\langle n^+|\delta\rangle$ ($G_n^E(t)$); (*e*) imaginary parts of $\langle n^+|\langle \hat{H}/J\rangle|D_1\rangle$ ($H_n^D(t)$) and $\langle n^+|\delta\rangle$ ($H_n^E(t)$); (*f*) real parts of $\langle n, 1|\hat{H}/J|D_1\rangle$ ($I_n^D(t)$) and $\langle n, 1|\delta\rangle$ ($I_n^E(t)$); (*g*) real parts of $\langle n, 5|\hat{H}/J|D_1\rangle$ ($J_n^D(t)$) and $\langle n, 5|\delta\rangle$ ($J_n^E(t)$).

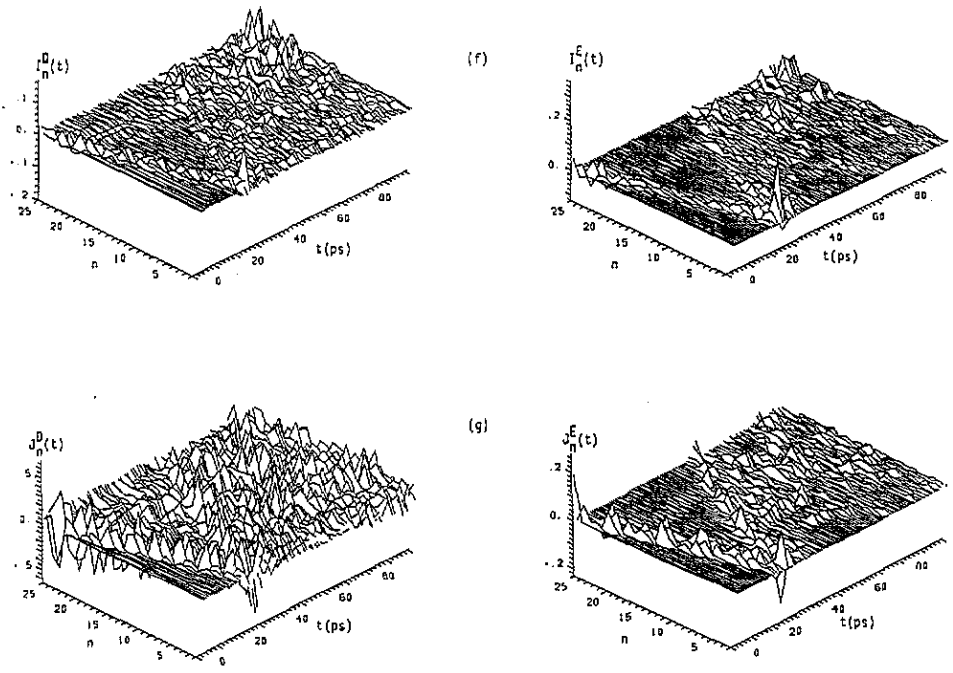

Figure 5. (Continued)

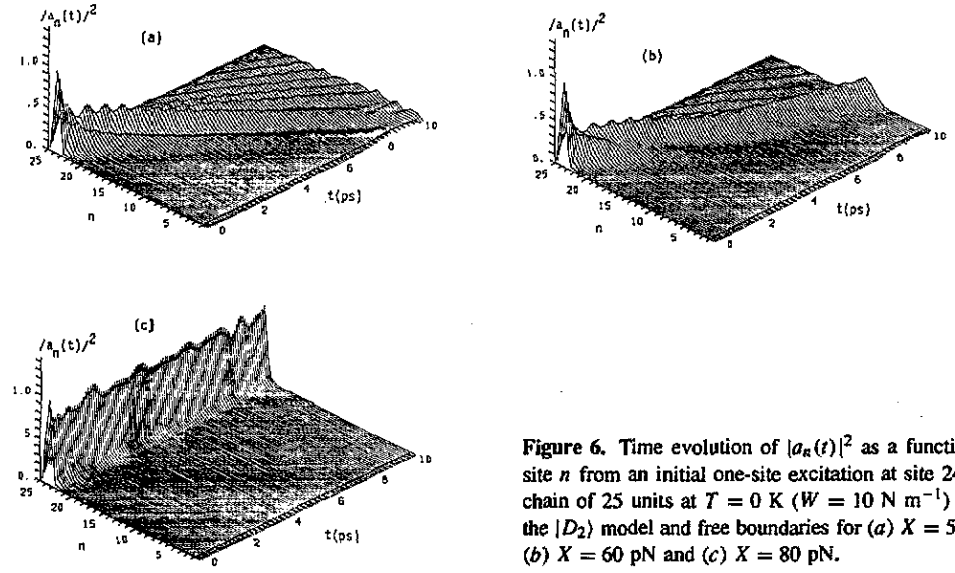

Figure 6. Time evolution of $|a_n(t)|^2$ as a function of site n from an initial one-site excitation at site 24 in a chain of 25 units at $T = 0$ K ($W = 10$ N m^{-1}) using the $|D_2\rangle$ model and free boundaries for (*a*) $X = 50$ pN, (*b*) $X = 60$ pN and (*c*) $X = 80$ pN.

but the difference is not tremendous (see below). One recognizes two differences between $|D_1\rangle$ and $|D_2\rangle$ immediately from the expressions in appendix 2. First of all the deviation state for the $|D_2\rangle$ model is not proportional to J, as it is in the $|D_1\rangle$ case, and thus $|D_2\rangle$ is not exact in the small-polaron limit ($J = 0$). Further the projection in the direction $|n\rangle = \hat{a}_n^+|0\rangle_e|\beta\rangle$ vanishes as in the $|D_1\rangle$ case but the additional deviations in the directions $|n^\pm\rangle = \hat{a}_n|0\rangle_e|\beta_{n\pm1}\rangle$ naturally cannot occur in $|D_2\rangle$ theory because such basis states are not

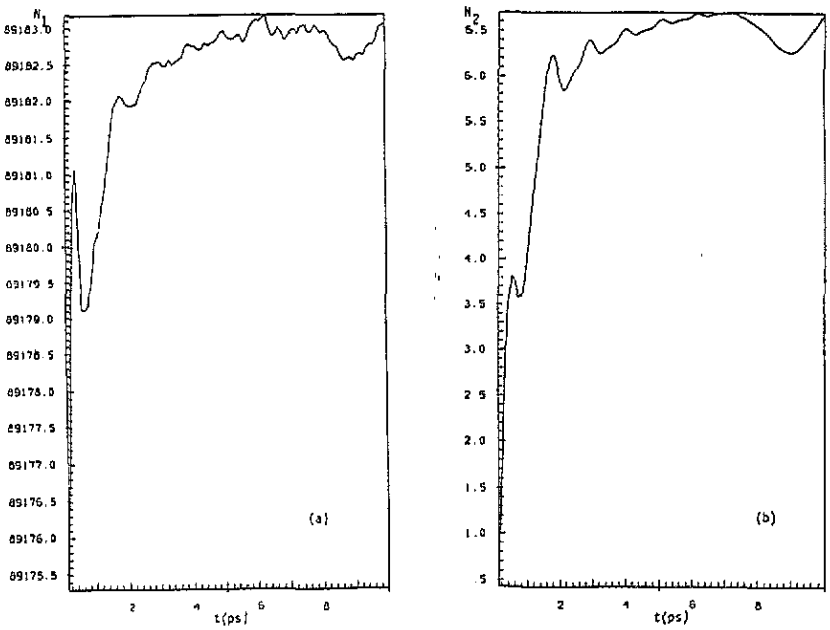

Figure 7. Time evolution of (*a*) the norm N_1 of the state $(H/J)|D_2\rangle$ and (*b*) the norm N_2 of the deviation $|\lambda\rangle$. The parameters are $W = 13$ N m^{-1}, and $X = 62$ pN.

present there.

In figure 7 we show for the $|D_2\rangle$ states the norms $\langle D_2|(\hat{H}/J)|D_2\rangle$ and $\langle\lambda|\lambda\rangle$ for the usually used parameter values $W = 13$ N m^{-1} and $X = 62$ pN and free-boundary conditions. From the figure we see that the two curves are nearly parallel and that the norm of the deviation is larger by a factor of about 3 than in the $|D_1\rangle$. case. While the norm of $(\hat{H}/J)|D_1\rangle$ spreads over a region of 110, the norm of $(\hat{H}/J)|D_2\rangle$ spreads over a region of roughly 5. This means that in the latter case the variation in the norm with time is completely governed by the time variation in the deviation which is by far not the case for the $|D_1\rangle$ state. Therefore already from these norms we can deduce that the time variation in $|D_1\rangle$ is much more accurate than that of $|D_2\rangle$.

In figure 8(*a*) we show the expectation values of the number operators of the amide-I oscillators in our two states. Although the deviation is somewhat larger than in the $|D_1\rangle$ case, this difference is not significant. This result is to be expected, because the deviation state in the $|D_2\rangle$ case has no coefficients on the basis states $|n\rangle$. For the momentum operators (figure 8(*b*)) the deviations are larger by a factor of 2 than in the $|D_1\rangle$ model, while in the case of the displacement operators they are of the same order of magnitude, but here the expectation values of the operators formed with the $(\hat{H}/J)|D_2\rangle$ state are much smaller than those formed with the $(\hat{H}/J)|D_1\rangle$ state and thus the errors in the $|D_2\rangle$ case are more significant, although still small. The reason that the deviations in the $|D_2\rangle$ model are also small is that they are minimized by the time-dependent variational principle also in this case. However, this must lead to results which differ from those of $|D_1\rangle$, because in the $|D_2\rangle$ case the basis space is much smaller.

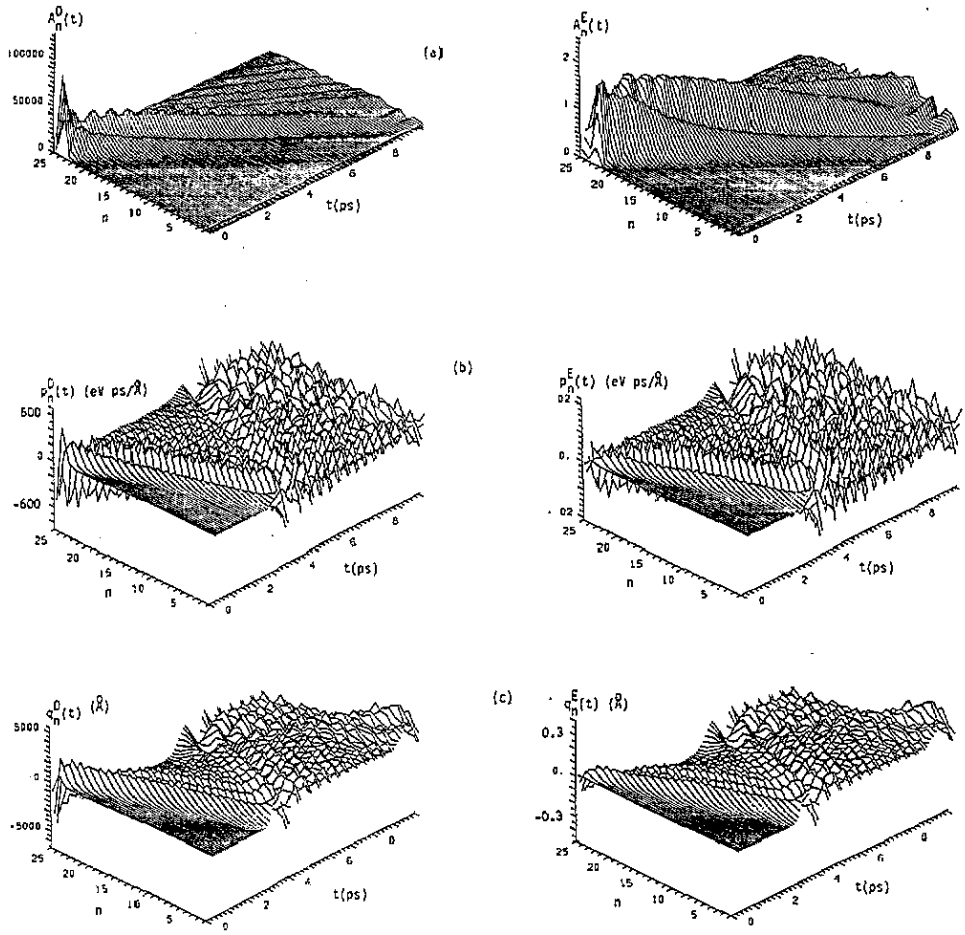

Figure 8. Expectation values of several operators in the state $(\hat{H}/J)|D_2\rangle$ (denoted by D), and in the deviation $|\lambda\rangle$ (denoted by E), computed in the $|D_2\rangle$ model ($W = 13$ N m^{-1}; $X = 62$ pN): (*a*) number operators $A_n^{\mathrm{D}}(t)$ and $A_n^{\mathrm{E}}(t)$ for the amide-I oscillators as functions of site n and time t; (*b*) momentum operators $p_n^{\mathrm{D}}(t)$ and $p_n^{\mathrm{E}}(t)$ as functions of site n and time t; (*c*) displacement operators $q_n^{\mathrm{D}}(t)$ and $q_n^{\mathrm{E}}(t)$ as functions of site n and time t.

4. Conclusion

We have numerically determined different expectation values formed with the $(\hat{H}/J)|D_1\rangle$ state and $|\delta\rangle$, which is the deviation from the exact solution of the time-dependent Schrödinger equation, i.e. for our approximation $[i\hbar(\partial/\partial t) - \hat{H}]|D_1\rangle = J|\delta\rangle$ holds. We found that, for all the expectation values that we computed, including the norm of the two states, those formed with $|\delta\rangle$ are completely negligible compared with those formed with $(\hat{H}/J)|D_1\rangle$. Although this is not a direct measure of the corresponding errors in the expectation values of operators formed with the $|D_1\rangle$ state, it gives at least an idea of the importance of the deviation. Thus we conclude that the $|D_1\rangle$ *ansatz* should give a relatively good approximation to the exact solutions, specifically since it is the exact solution in the small polaron limit ($J = 0$). This is not the case for the $|D_2\rangle$ *ansatz*, although the corresponding deviation there also results in rather small expectation values. Therefore it is clear that the basis space in the $|D_2\rangle$ case is too limited and one has to conclude

that here the time-dependent variational principle must result in solutions which are even qualitatively different from the exact solutions in order to minimize the deviation, since the small-polaron limit is also not reproduced. On the other hand the extended basis space of the $|D_1\rangle$ state is sufficient to reproduce the small-polaron limit, which leads to the conclusion that solutions other than $J = 0$ have to be at least qualitatively correct. This conclusion is supported by the numerical results from the deviation state in this case. Further the error evolves proportional to J from the exact small-polaron case and the actual value of J is small (0.967 meV). Also projections of the deviation in the directions of the basis states are negligible for all basis states which have a large contribution in $(\hat{H}/J)|D_1\rangle$, while only for basis states which are already negligible in $(\hat{H}/J)|D_1\rangle$ is the error comparable with the contribution in $(\hat{H}/J)|D_1\rangle$.

However, it is desirable to have a better *ansatz* state than $|D_1\rangle$. Comparison of the results obtained with such a state with $|D_1\rangle$ results would give final justification for the use of the $|D_1\rangle$ approximation. In appendix 3, on the basis of the considerations of Mechtly and Shaw [15], we outline a strategy of how one can obtain such an improved *ansatz*. Work along this line is in progress in our laboratory.

Acknowledgments

The financial support of the Deutsche Forschungsgemeinschaft (project Fo 175/2-3) and of the Fonds der Chemischen Industrie is gratefully acknowledged.

Appendix 1. Commutation relations and expectation values

The well known commutation relations for boson operators are

$$\hat{b}_k\hat{b}_{k'}^+ = \hat{b}_{k'}^+\hat{b}_k + \delta_{kk'}. \tag{A1.1}$$

From this, one can easily show by complete induction that

$$\begin{aligned}\hat{b}_k(\hat{b}_k^+)^m &= (\hat{b}_k^+)^m\hat{b}_k + m(\hat{b}_k^+)^{m-1}\\ \hat{b}_k^+(\hat{b}_k)^m &= (\hat{b}_k)^m\hat{b}_k^+ - m(\hat{b}_k)^{m-1}.\end{aligned} \tag{A1.2}$$

Further we have for the displacement operators

$$\hat{U}_{nk} = \exp(b_{nk}\hat{b}_k^+ - b_{nk}^*\hat{b}_k) = \exp(-\tfrac{1}{2}|b_{nk}|^2)\exp(b_{nk}\hat{b}_k^+)\exp(-b_{nk}^*b_k). \tag{A1.3}$$

As an example of how to proceed we compute two of the necessary commutators:

$$\begin{aligned}\hat{b}_k\hat{U}_{nk} &= \exp(-\tfrac{1}{2}|b_{nk}|^2)\sum_{\nu=0}^{\infty}\frac{b_{nk}^\nu}{\nu!}\hat{b}_k(\hat{b}_k^+)^\nu\exp(-b_{nk}^*\hat{b}_k)\\ &= \exp(-\tfrac{1}{2}|b_{nk}|^2)\left(\sum_{\nu=1}^{\infty}\frac{b_{nk}^\nu}{\nu!}\nu(\hat{b}_k^+)^{\nu-1} + \sum_{\nu=0}^{\infty}\frac{b_{nk}^\nu}{\nu!}(\hat{b}_k^+)^\nu\hat{b}_k\right)\exp(-b_{nk}^*\hat{b}_k)\\ &= \exp(-\tfrac{1}{2}|b_{nk}|^2)\left(b_{nk}\sum_{\nu=1}^{\infty}\frac{b_{nk}^{\nu-1}}{(\nu-1)!}(\hat{b}_k^+)^{\nu-1} + \exp(b_{nk}\hat{b}_k^+)\hat{b}_k\right)\exp(-b_{nk}^*\hat{b}_k)\\ &= \exp(-\tfrac{1}{2}|b_{nk}|^2)\exp(b_{nk}\hat{b}_k^+)\exp(-b_{nk}*\hat{b}_k)(b_{nk}+\hat{b}_k) = \hat{U}_{nk}(\hat{b}_k + b_{nk}).\end{aligned} \tag{A1.4}$$

Thus we obtain finally that

$$\hat{b}_k \hat{U}_n = \hat{U}_n(\hat{b}_k + b_{nk}). \tag{A1.5}$$

In complete analogy we calculate

$$\hat{b}_k^+ \hat{U}_{nk} = \exp(-\tfrac{1}{2}|b_{nk}|^2)\exp(b_{nk}\hat{b}_k^+)\left(\sum_{\nu=0}^{\infty}\frac{(-b_{nk}^*)^\nu}{\nu!}\hat{b}_k^\nu\hat{b}_k^+ - (-b_{nk}^*)\sum_{\nu=1}^{\infty}\frac{(-b_{nk}^*)^{\nu-1}}{(\nu-1)!}\hat{b}_k^{\nu-1}\right)$$

$$= \hat{U}_{nk}(\hat{b}_k^+ + b_{nk}^*) \tag{A1.6}$$

and thus

$$\hat{b}_k^+ \hat{U}_n = \hat{U}_n(\hat{b}_k^+ + b_{nk}^*). \tag{A1.7}$$

From this all the necessary expressions can be easily obtained:

$$\begin{aligned}
&\hat{b}_k \hat{U}_n = \hat{U}_n(\hat{b}_k + b_{nk}) && \hat{b}_k^+ \hat{U}_n = \hat{U}_n(\hat{b}_k^+ + b_{nk}^*)\\
&\hat{U}_n \hat{b}_k = (\hat{b}_k - b_{nk})\hat{U}_n && \hat{U}_n \hat{b}_k^+ = (\hat{b}_k^+ - b_{nk}^*)\hat{U}_n\\
&\hat{U}_n^+ \hat{b}_k^+ = (\hat{b}_k^+ + b_{nk}^*)\hat{U}_n^+ && \hat{U}_n^+ \hat{b}_k = (\hat{b}_k + b_{nk})\hat{U}_n^+\\
&\hat{b}_k^+ \hat{U}_n^+ = \hat{U}_n^+(\hat{b}_k^+ - b_{nk}^*) && \hat{b}_k \hat{U}_n^+ = \hat{U}_n^+(\hat{b}_k - b_{nk}).
\end{aligned} \tag{A1.8}$$

With the help of these expressions and of

$$\langle\beta_n|\hat{b}_k|\beta_m\rangle = b_{mk}D_{nm} \qquad \langle\beta_n|\hat{b}_k^+|\beta_m\rangle = b_{nk}^* D_{nm} \tag{A1.9}$$

we can compute the following expectation values which are needed for the calculations described in the main text:

$$\langle\beta_m|\hat{U}_n\hat{b}_k^+|0\rangle_{\mathrm{p}} = (b_{mk}^* - b_{nk}^*)D_{mn} = ({}_{\mathrm{p}}\langle 0|\hat{b}_k\hat{U}_n^+|\beta_m\rangle)^* \tag{A1.10}$$

$$\begin{aligned}
&\langle\beta_n|\hat{b}_k\hat{U}_m\hat{b}_{k'}^+|0\rangle_{\mathrm{p}} = [\delta_{kk'} + (b_{nk'}^* - b_{mk'}^*)b_{mk}]D_{nm}\\
&\langle\beta_n|\hat{b}_k^+\hat{U}_m\hat{b}_{k'}^+|0\rangle_{\mathrm{p}} = (b_{nk'}^* - b_{mk'})b_{nk}^* D_{nm}
\end{aligned} \tag{A1.11}$$

$$\begin{aligned}
&{}_{\mathrm{p}}\langle 0|\hat{b}_{k'}\hat{U}_n^+\hat{b}_k^+|\beta_m\rangle = [\delta_{kk'} + (b_{mk'} - b_{nk'})b_{nk}^*]D_{nm}\\
&{}_{\mathrm{p}}\langle 0|\hat{b}_{k'}\hat{U}_n^+\hat{b}_k|\beta_m\rangle = (b_{mk'} - b_{nk'})b_{mk}D_{nm}
\end{aligned} \tag{A1.12}$$

$${}_{\mathrm{p}}\langle 0|\hat{b}_k\hat{U}_n^+\hat{U}_n\hat{b}_{k'}^+|0\rangle_{\mathrm{p}} = \delta_{kk'} \tag{A1.13}$$

$${}_{\mathrm{p}}\langle 0|\hat{b}_{k'}\hat{U}_n^+\hat{b}_k\hat{U}_n\hat{b}_{k''}^+|0\rangle_{\mathrm{p}} = b_{nk}\delta_{k'k''} = ({}_{\mathrm{p}}\langle 0|\hat{b}_{k'}\hat{U}_n^+\hat{b}_k^+\hat{U}_n\hat{b}_{k''}^+|0\rangle_{\mathrm{p}})^*. \tag{A1.14}$$

To demonstrate the way in which to compute these expectation values we shall give just two examples:

$${}_{\mathrm{p}}\langle 0|\hat{b}_{k'}\hat{U}_n^+\hat{b}_k^+|\beta_m\rangle = {}_{\mathrm{p}}\langle 0|\hat{U}_n^+(\hat{b}_{k'} - b_{nk'})\hat{b}_k^+|\beta_m\rangle = \langle\beta_n|\hat{b}_{k'}\hat{b}_k^+|\beta_m\rangle - \langle\beta_n|\hat{b}_k^+|\beta_m\rangle b_{nk'}$$

$$= \langle\beta_n|\delta_{kk'} + \hat{b}_k^+\hat{b}_{k'}|\beta_m\rangle - b_{nk}^* b_{nk'}D_{nm} = [\delta_{kk'} + (b_{mk'} - b_{nk'})b_{nk}^*]D_{nm} \tag{A1.15}$$

$${}_{\mathrm{p}}\langle 0|\hat{b}_{k'}\hat{U}_n^+\hat{b}_k|\beta_m\rangle = {}_{\mathrm{p}}\langle 0|\hat{b}_{k'}\hat{U}_n^+|\beta_m\rangle b_{mk} = {}_{\mathrm{p}}\langle 0|\hat{U}_n^+(\hat{b}_{k'} - b_{nk'})|\beta_m\rangle b_{mk}$$

$$= \langle\beta_n|\hat{b}_{k'}|\beta_m\rangle b_{mk} - \langle\beta_n|\beta_m\rangle b_{nk'}b_{mk} = (b_{mk'} - b_{nk'})b_{mk}D_{nm}. \tag{A1.16}$$

Besides the commutation rules, for these calculations one has to use the fact that the coherent states are eigenfunctions of the annihilation operator:

$$\hat{b}_k|\beta_n\rangle = b_{nk}|\beta_n\rangle \qquad \langle\beta_n|\hat{b}_k^+ = \langle\beta_n|b_{nk}^*. \tag{A1.17}$$

Finally we use that

$$\hat{a}_n\hat{a}_m^+ = \hat{a}_m^+\hat{a}_n + \delta_{nm} \rightarrow {}_{\mathrm{e}}\langle 0|\hat{a}_n\hat{a}_m^+|0\rangle_{\mathrm{e}} = \delta_{nm} \qquad {}_{\mathrm{e}}\langle 0|\hat{a}_n\hat{a}_i^+\hat{a}_i\hat{a}_m^+|0\rangle_{\mathrm{e}} = \delta_{ni}\delta_{mi}. \tag{A1.18}$$

Appendix 2. Expressions for the $|D_2\rangle$ approximation

For comparison we wish to derive the error in the simpler $|D_2\rangle$ *ansatz*, in which the lattice is described classically. The *ansatz* is given by

$$|D_2\rangle = \sum_n a_n(t)\hat{a}_n^+|0\rangle_e|\beta\rangle$$
$$|\beta\rangle = \hat{U}|0\rangle_p = \exp\left(\sum_k [b_k(t)b_k^+ - b_k^*(t)\hat{b}_k]\right)|0\rangle_p. \tag{A2.1}$$

We see that here the manifold of basis states $|\beta_n\rangle$ for the description of the lattice displacements is reduced to a single basis state $|\beta\rangle$. With a straightforward derivation we obtain

$$L_t = \tfrac{1}{2}i\hbar[\langle D_2|(\partial/\partial t)D_2\rangle - \langle(\partial/\partial t)D_2|D_2\rangle]$$
$$= \tfrac{1}{2}i\hbar\left[\sum_n(\dot{a}_n a_n^* - a_n\dot{a}_n^*) + \left(\sum_n |a_n|^2\right)\sum_k(\dot{b}_k b_k^* - b_k\dot{b}_k^*)\right]. \tag{A2.2}$$

Together with the expectation value of the Hamiltonian this gives the Lagrange function

$$L = L_t - \langle D_2|\hat{H}|D_2\rangle = \tfrac{1}{2}i\hbar\sum_n(\dot{a}_n a_n^* - a_n\dot{a}_n^*) + \tfrac{1}{2}i\hbar\sum_{nk}|a_n|^2(\dot{b}_k b_k^* - b_k\dot{b}_k^*)$$
$$- \sum_n[E_0|a_n|^2 - Ja_n^*(a_{n+1} + a_{n-1}) - \sum_{nk}\hbar\omega_k[|b_k|^2 + \tfrac{1}{2} + B_{nk}(b_k + b_k^*)]|a_n|^2. \tag{A2.3}$$

The Euler–Lagrange equations for a_n lead to

$$i\hbar\dot{a}_n = \left(E_0 + \tfrac{1}{2}\sum_k\hbar\omega_k\right)a_n - \tfrac{1}{2}i\hbar\sum_k(\dot{b}_k b_k^* - b_k\dot{b}_k^*)a_n$$
$$- J(a_{n+1} + a_{n-1}) + \sum_k\hbar\omega_k[|b_k|^2 + B_{nk}(b_k + b_k^*)]a_n. \tag{A2.4}$$

From this, one can show that the norm is conserved, i.e.

$$\frac{d}{dt}\sum_n|a_n|^2 = 0 \rightarrow \sum_n|a_n(t)|^2 = \sum_n|a_n(t=0)|^2 = 1. \tag{A2.5}$$

With (A2.5) and the Euler–Lagrange equations for the b-values we obtain the equations of motion

$$i\hbar\dot{b}_k = \hbar\omega_k\left(b_k + \sum_n B_{nk}|a_n|^2\right) \tag{A2.6}$$

which can be shown to be equivalent to the more familiar equations

$$\dot{p}_n = W(q_{n+1} - 2q_n + q_{n-1}) + X(|a_n|^2 - |a_{n-1}|^2). \tag{A2.7}$$

This leads to the final equations for the a-values:

$$i\hbar\dot{a}_n = \left(E_0 + \tfrac{1}{2}\sum_k\hbar\omega_k\right)a_n - J(a_{n+1} + a_{n-1}) + \sum_k\hbar\omega_k\left(B_{nk} - \tfrac{1}{2}\sum_m B_{mk}|a_m|^2\right)(b_k^* + b_k)a_n \tag{A2.8}$$

equivalent to

$$i\hbar\dot{a}_n = \left(E_0+\tfrac{1}{2}\sum_k \hbar\omega_k\right)a_n - J(a_{n+1}+a_{n-1}) + X(q_{n+1}-q_n)a_n - \tfrac{1}{2}X\sum_m |a_m|^2(q_{m+1}-q_m)a_n. \tag{A2.9}$$

With the gauge transformation

$$a_n(t) = A_n(t)\exp\left\{\frac{i}{\hbar}\left[-\left(E_0+\tfrac{1}{2}\sum_k\hbar\omega_k\right)t + \tfrac{1}{2}X\sum_m\int_0^t |a_m(t')|^2[q_{m+1}(t')-q_m(t')]\,dt'\right]\right\} \tag{A2.10}$$

this can be transformed into the familiar form

$$i\hbar\dot{A}_n = -J(A_{n+1}+A_{n-1}) + X(q_{n+1}-q_n)A_n. \tag{A2.11}$$

Note that, with Davydov's method for the derivation of the equations of motion (treating $\langle D_2|\hat{H}|D_2\rangle$ as the classical Hamiltonian function), equation (A2.11) is obtained; however, the second term in the phase in equation (A2.10) is missing. Now again we can compute $i\hbar(\partial/\partial t)|D_2\rangle$ and $\hat{H}|D_2\rangle$ separately and we obtain

$$i\hbar(\partial/\partial t)|D_2\rangle = J[(H/J)|D_2\rangle + |\lambda\rangle]. \tag{A2.12}$$

We introduce the state

$$\begin{aligned} &|\chi\rangle = \sum_n \gamma_n|n\rangle + \sum_{nk}\alpha_{nk}|n,k\rangle \\ &|n\rangle = \hat{a}_n^+|0\rangle_e|\beta\rangle \qquad |n,k\rangle = \hat{a}_n^+|0\rangle_e\hat{U}\hat{b}_k^+|0\rangle_p \\ &\langle n|m\rangle = \delta_{nm} \qquad \langle n|m,k\rangle = 0 \qquad \langle n,k|m,k'\rangle = \delta_{nm}\delta_{kk'}. \end{aligned} \tag{A2.13}$$

We obtain $|\chi\rangle = |\lambda\rangle$ if we set

$$\begin{aligned} &\gamma_n = 0 \\ &\alpha_{nk} = \frac{\hbar\omega_k}{J}\left(\sum_m |a_m|^2 B_{mk} - B_{nk}\right)a_n \end{aligned} \tag{A2.14}$$

and further $|\chi\rangle = (\hat{H}/J)|D_2\rangle$ if we set

$$\begin{aligned} &\gamma_n = \frac{1}{J}\sum_n\left[\left(E_0 + \sum_k \hbar\omega_k[|b_k|^2 + \tfrac{1}{2} + B_{nk}(b_k^* + b_k)]\right)a_n - J(a_{n+1}+a_{n-1})\right] \\ &\alpha_{nk} = (\hbar\omega_k/J)(b_k + B_{nk})a_n. \end{aligned} \tag{A2.15}$$

The projections on the basis states are, because of their orthogonality in this case, simply

$$\langle n|\chi\rangle = \gamma_n \qquad \langle n,k|\chi\rangle = \alpha_{nk} \tag{A2.16}$$

and our expectation values are

$$\begin{aligned}
&\langle\chi|\chi\rangle = \sum_n |\gamma_n|^2 + \sum_{nk} |\alpha_{nk}|^2 \\
&\langle\chi|\hat{a}_n^+\hat{a}_n|\chi\rangle = |\gamma_n|^2 + \sum_k |\alpha_{nk}|^2 \\
&\langle\chi|\hat{b}_k|\chi\rangle = \sum_n \gamma_n^*(\gamma_n b_k + \alpha_{nk}) + b_k \sum_{nk'} |\alpha_{nk'}|^2 = (\langle\chi|\hat{b}_k^+|\chi\rangle)^* \\
&\langle\chi|\hat{q}_n|\chi\rangle = \sqrt{\frac{2\hbar}{M}} \sum_k \frac{U_{nk}}{\sqrt{\omega_k}} \mathrm{Re}(\langle\chi|\hat{b}_k|\chi\rangle) \\
&\langle\chi|\hat{p}_n|\chi\rangle = \sqrt{2\hbar M} \sum_k \sqrt{\omega_k} U_{nk} \,\mathrm{Im}(\langle\chi|\hat{b}_k|\chi\rangle).
\end{aligned} \tag{A2.17}$$

Appendix 3. Improved *ansatz* including two-phonon terms

Mechtly and Shaw [15] have shown that the exact solution $|\psi(t)\rangle$ of the Schrödinger equation can be written in the form

$$|\psi(t)\rangle = \sum_n a_n(t)\hat{a}_n^+|0\rangle_e \hat{W}_n|0\rangle_p \tag{A3.1}$$

where

$$\hat{W}_n = \exp\hat{S}_n. \tag{A3.2}$$

The anti-Hermitian generator $\hat{S}_n$ can be expanded into an infinite series of normal ordered products of arbitrary numbers of phonon creation and annihilation operators multiplied by time-dependent coefficients:

$$\begin{aligned}
\hat{S}_n(t) = &\sum_k [b_{nk}(t)\hat{b}_k^+ - b_{nk}^*(t)\hat{b}_k] - \sum_{kk'} f_{kk',n}(t)\hat{b}_k^+\hat{b}_{k'} \\
&+ \tfrac{1}{2}\sum_{kk'} [g_{kk',n}(t)\hat{b}_k^+\hat{b}_{k'}^+ - g_{kk',n}^*(t)\hat{b}_k\hat{b}_{k'}] + \ldots.
\end{aligned} \tag{A3.3}$$

We see that a truncation of the series after the first term leads to the $|D_1\rangle$ state. In this first term it is taken into account that an amide-I excitation at unit n can create or annihilate a phonon of the normal mode k. However, the normal modes remain uncoupled since only one-phonon processes are included. In the second sum it is taken into account that a phonon with wavenumber k' can be annihilated by the creation of another phonon with wavenumber k, while the third sum describes the simultaneous creation or annihilation of two phonons with wavenumber k and k'. The higher-order terms then include three-phonon processes, four-phonon processes, and so on. The convergence of the series can probably be investigated only numerically.

In a first attempt to study this convergence and to improve the quality of the *ansatz* beyond $|D_1\rangle$ we are planning to take the two two-phonon processes into account. For this purpose we have to derive the Lagrangian

$$L = \langle\psi(t)|\tfrac{1}{2}i\hbar\frac{\partial^{\leftrightarrow}}{\partial t} - \hat{H}|\psi(t)\rangle \tag{A3.4}$$

from which with the help of the Euler–Lagrange equations

$$(\mathrm{d}/\mathrm{d}t)(\partial L/\partial \dot{\varphi}_\mu^*) - \partial L/\partial \varphi_\mu^* = 0 \qquad \varphi_\mu = a_n,\ b_{nk},\ f_{kk',n} \text{ or } g_{kk',n} \tag{A3.5}$$

the $2N^3 + N^2 + N$ complex equations of motion can be obtained and solved numerically. Work along this line is in progress in our laboratory and the results will be the subject of a future paper.

However, one should also still seek temperature models which lead to quantitatively more reliable results than the average Hamiltonian model, although the latter model is qualitatively correct [5]. For this purpose, one could start with the usual initial state

$$|\psi_\nu(t=0)\rangle = \sum_n a_n(t=0)\hat{a}_n^+|0\rangle_e|\nu\rangle \qquad |\nu\rangle = \prod_k \frac{1}{\sqrt{\nu_k!}}(\hat{b}_k^+)^{\nu_k}|0\rangle_p \tag{A3.6}$$

where ν denotes one of the possible phonon distributions in the lattice. Then at time t the exact state is given by

$$|\psi_\nu(t)\rangle = \exp[-(\mathrm{i}/\hbar)\hat{H}t]|\psi_\nu(t=0)\rangle. \tag{A3.7}$$

The expectation value of an operator $\hat{A}$, where in our case the exciton number operators and phonon and exciton annihilation operators are of interest, computed for our state is given as

$$A_\nu(t) = \langle\psi_\nu(t)|\hat{A}|\psi_\nu(t)\rangle = \langle\psi_\nu(t=0)|\exp[(\mathrm{i}/\hbar)\hat{H}t]\hat{A}\exp[(-\mathrm{i}/\hbar)\hat{H}t]|\psi_\nu(t=0)\rangle. \tag{A3.8}$$

A thermal average finally gives the expectation value at time t and temperature T:

$$A(t) = \sum_\nu \rho_\nu A_\nu(t) \qquad \rho_\nu = \langle\nu|\exp\left(-\frac{\hat{H}_p}{k_B T}\right)|\nu\rangle \Big/ \sum_\mu \langle\mu|\exp\left(-\frac{\hat{H}_p}{k_B T}\right)|\mu\rangle \tag{A3.9}$$

where $\hat{H}_p$ is the phonon part of the Davydov Hamiltonian. Expansion of the exponentials results in the final equation

$$A(t) = \sum_\nu \rho_\nu \sum_{kl} \frac{(\mathrm{i}/\hbar)^{k+l}(-1)^l}{k!l!}\langle\psi_\nu(t=0)|\hat{H}^k\hat{A}\hat{H}^l|\psi_\nu(t=0)\rangle t^{k+l}. \tag{A3.10}$$

Thus one has to compute commutators of the kind

$$[\hat{A}, \hat{H}] \qquad [\hat{A}, \hat{H}^l]. \tag{A3.11}$$

It is hoped that a closed form for the expressions can be found or, if this is not possible, the expansion of the exponentials can be truncated after a suitable number of terms. Work along these lines is in progress in our laboratory.

References

[1] Davydov A S and Kislukha N I 1973 *Phys. Status Solidi* b **59** 465
Davydov A S 1979 *Phys. Scr.* **20** 387

[2] Davydov A S 1980 *Zh. Eksp. Teor. Fiz.* **78** 789 (Engl. Trans. 1980 *Sov. Phys.–JETP* **51** 397)

[3] Scott A C 1982 *Phys. Rev.* A **26** 57; 1984 *Phys. Scr.* **29** 279
MacNeil L and Scott A C 1984 *Phys. Scr.* **29** 284; 1985 *Phil. Trans. R. Soc.* A **315** 423

[4] Förner W and Ladik J 1991 *Davydov's Soliton Revisited (NATO ASI Series B, 243)* ed P L Christiansen and A C Scott (New York: Plenum) p 267

[5] Förner W 1993 *J. Phys.: Condens. Matter* **5** 803
[6] Halding J and Lomdahl P S 1987 *Phys. Lett.* **124A** 37
[7] Lomdahl P S and Kerr W C 1985 *Phys. Rev. Lett.* **55** 1235; 1991 *Davydov's Soliton Revisited (NATO ASI Series B, 243)* ed P L Christiansen and A C Scott (New York: Plenum)
Kerr W C and Lomdahl P S 1987 *Phys. Rev.* B **35** 3629
Kerr W C and Lomdahl P S 1991 *Davydov's Soliton Revisited (NATO ASI Series B, 243)* ed P L Christiansen and A C Scott (New York: Plenum)
[8] Lawrence A F, McDaniel J C, Chang D B, Pierce B M and Birge R R 1986 *Phys. Rev.* A **33** 1188
[9] Bolterauer H 1986 *Structure Coherence and Chaos, Proc. MIDIT 1986 Workshop* (Manchester: Manchester University Press); 1991 *Davydov's Soliton Revisited (NATO ASI Series B, 243)* ed P L Christiansen and A C Scott (New York: Plenum)
[10] Cottingham J P and Schweitzer J W 1989 *Phys. Rev. Lett.* **62** 1792
Schweitzer J W and Cottingham J P 1991 *Davydov's Soliton Revisited (NATO ASI Series B, 243)* ed P L Christiansen and A C Scott (New York: Plenum)
[11] Motschmann H, Förner W and Ladik J 1989 *J. Phys.: Condens. Matter* **1** 5083
[12] Förner W 1991 *J. Phys.: Condens. Matter* **3** 4333; 1992 *J. Comput. Chem.* **13** 275
[13] Brown D W, Lindenberg K and West B J 1986 *Phys. Rev.* A **33** 4104, 4110; 1987 *Phys. Rev.* B **35** 6169; 1988 *Phys. Rev.* B **37** 2946
Brown D W 1988 *Phys. Rev.* A **37** 5010
[14] Cruzeiro L, Halding J, Christiansen P L, Skovgaard O and Scott A C 1988 *Phys. Rev.* A **37** 880
[15] Mechtly B and Shaw P B 1985 *Phys. Rev.* B **38** 3075
[16] Skrinar J, Kapor D V and Stojanovic S D 1988 *Phys. Rev.* A **38** 6402
[17] Förner W 1991 *Phys. Rev.* A **44** 2694; 1993 *J. Mol. Struct.* at press
[18] Förner W 1992 *Nanobiology* **1** 413
[19] Förner W 1992 *J. Phys.: Condens. Matter* **4** 1915
[20] Wang X, Brown D W and Lindenberg K 1989 *Phys. Rev. Lett.* **62** 1796
[21] Scott A C 1990 *Conference on Nonlinear Sciences: The Next Decade (Los Alamos National Laboratory 21 May 1990)*
[22] Brown D W and Ivic Z 1989 *Phys. Rev.* B **40** 9876
[23] Scott A C 1992 *Phys. Rep.* **217** 1
[24] Schweitzer J P 1993 *Phys. Rev.* A at press
[25] Förner W 1993 *J. Phys.: Condens. Matter* **5** 823
[26] Förner W 1993 *J. Phys.: Condens. Matter* **5** 3883–96